Interface and surface stabilization of the polarization in ferroelectric thin films

Chiara Gattinoni[a,1], Nives Strkalj[a], Rea Härdi[a], Manfred Fiebig[a], Morgan Trassin[a], and Nicola A. Spaldin[a]

[a]Department of Materials, ETH Zurich, 8093 Zurich, Switzerland

Edited by Angel Rubio, Max Planck Institute for the Structure and Dynamics of Matter, Hamburg, Germany, and approved September 21, 2020 (received for review April 21, 2020)

Ferroelectric perovskites present a switchable spontaneous polarization and are promising energy-efficient device components for digital information storage. Full control of the ferroelectric polarization in ultrathin films of ferroelectric perovskites needs to be achieved in order to apply this class of materials in modern devices. However, ferroelectricity itself is not well understood in this nanoscale form, where interface and surface effects become particularly relevant and where loss of net polarization is often observed. In this work, we show that the precise control of the structure of the top surface and bottom interface of the thin film is crucial toward this aim. We explore the properties of thin films of the prototypical ferroelectric lead titanate ($PbTiO_3$) on a metallic strontium ruthenate ($SrRuO_3$) buffer using a combination of computational (density functional theory) and experimental (optical second harmonic generation) methods. We find that the polarization direction and strength are influenced by chemical and electronic processes occurring at the epitaxial interface and at the surface. The polarization is particularly sensitive to adsorbates and to surface and interface defects. These results point to the possibility of controlling the polarization direction and magnitude by engineering specific interface and surface chemistries.

thin films | critical thickness | ferroelectricity | surface science

The switchable spontaneous polarization of ferroelectric (FE) materials makes them very interesting for technological applications. Indeed, they are widely used in electronics and information technology as capacitors, ultrasonic transducers, thermistors, optoelectronic devices, and piezoelectric sensors (1, 2). In order to meet size requirements for miniaturized technological devices, the FE polarization of nanoscale-size (thin) films needs to be controlled. Despite advances in the theory of FE thin films (3–6), much is still to be understood.

There are multiple reasons why obtaining complete control of ferroelectricity at the nanoscale is a challenging task (7). First, below a certain thickness, the FE polarization becomes compromised as it is suppressed by the depolarizing field (8, 9). In addition, with decreasing thickness, surface and interface effects become increasingly important and can affect both the strength and direction of the polarization.

Screening of the depolarizing field at an interface is generally achieved by using a metal buffer to the insulating substrate material (10, 11). Since the screening of the polarization is not perfect, the buffer can generally not completely prevent the existence of a critical thickness (12). It has, however, been proposed that a robust polarization in ultrathin films—thinner than 30 unit cells (u.c.)—can be promoted by interface defects (13, 14), distortions in the metallic buffer (15, 16), or the interfacial chemical bonding (17–19). Interface effects can also influence the character of the polarization across the whole film in the ultrathin regime. For example, the chemical and electronic character of the interface between the FE and the buffer can determine the direction of the polarization in the film (20, 21). Indeed, different terminations of some ABO_3 perovskite buffers [BO_2 or AO in the (001) direction] have been observed to promote opposite polarization directions of a FE grown on its surface. Competing effects arising from the two interfaces in a heterostructure can also lead to domain walls across the FE film thickness as observed in $KNbO_3/SrRuO_3$ (22).

The presence of a surface adds further electrostatic and chemical considerations, namely, the polar discontinuity at the surface (4) and the charge compensation mechanisms required in order to avoid it. A robust compensation mechanism is vital for the stability of the ferroelectricity as the absence of sufficient compensating charge can trigger the formation of FE domains or the rotation of the polarization into the plane of the thin FE film (23). These effects are undesirable in many applications (24). In a stoichiometric FE/vacuum interface, compensation is expected to occur through an electronic reconstruction leading to a metallic surface; for a surface in contact with a nonvacuum environment, stoichiometry-altering mechanisms, including molecular adsorption or surface defect formation, are available (25, 26). Calculations suggest that passivation with ions is usually energetically favored over the metallization of the surface, and thus, nonstoichiometry is an effective way to provide the required electron and hole screening of the surface bound charges (3, 27, 28). Nonstoichiometry (5, 6, 29) and molecular adsorption (30, 31) can also lead to the reversal of the FE polarization and can change the Curie temperature (6). The stabilization of the FE polarization against surface effects is especially relevant in emerging applications such as catalysis (2), where interactions with the environment, such as humidity or chemicals present in the atmosphere, routinely occur.

It is thus clear that in order to engineer stable ferroelectricity in a thin film, interface and surface effects play a pivotal role.

Significance

With an ever-increasing societal demand for energy for electronic devices and in the face of the current climate issues, the need for low-energy-consuming electronics has never been greater. Ferroelectrics are promising energy-efficient device components for digital information storage, with the functionality relying on the manipulation of their polarization in ultrathin films. Polar discontinuities at the thin film interfaces and surfaces, however, can cause loss of polarization and thus functionality. Here we show how the interface and surface influence the overall polarization of the thin film. We show that the structure of the interface and surface can be tailored toward a specific polarization direction and strength, and that great control in the engineering of ferroelectrics thin films can be achieved.

Author contributions: C.G., M.F., M.T., and N.A.S. designed research; C.G., N.S., and R.H. performed research; and C.G., N.S., R.H., M.F., M.T., and N.A.S. wrote the paper.

The authors declare no competing interest.

This article is a PNAS Direct Submission.

[1]To whom correspondence may be addressed. Email: chiara.gattinoni@mat.ethz.ch.

This article contains supporting information online at https://www.pnas.org/lookup/suppl/doi:10.1073/pnas.2007736117/-/DCSupplemental.

First published October 29, 2020.

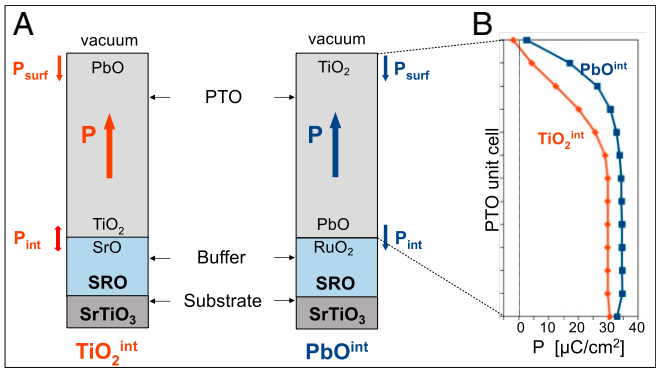

Fig. 1. (*A*) SRO/PTO/vacuum thin film geometries considered in this work. The TiO_2^{int} system (*Left*) has an SrO–TiO_2 interface and a PbO surface, and the PbO^{int} system (*Right*) has a RuO_2–PbO interface and a TiO_2 surface. P indicates the preferred direction of the FE polarization for the fully relaxed system. P_{int} and P_{surf} show the preferred polarization direction of the interface and the surface chemistry, respectively. (*B*) u.c. by u.c. polarization in a relaxed 13 u.c. film of PTO for the two SRO/PTO/vacuum systems. The interface is at the bottom, and the surface is at the top. The relaxed polarization direction is P_{up} in all cases.

However, the relative role of surface, interface, and electrostatic properties still needs to be clearly disentangled and well understood. In this work we address this problem. We investigate how the interface with the metallic buffer and the surface affect the FE polarization and how are they affected by nonstoichiometry. We achieve this by means of ab initio computational methods based on density functional theory (DFT) and by in situ second harmonic generation (ISHG) experiments which track the polarization during the pulsed-laser deposition (PLD) of a thin film (21, 32). We investigate with both approaches a lead titanate ($PbTiO_3$, PTO) thin film with a metallic strontium ruthenate ($SrRuO_3$, SRO) buffer grown on a strontium titanate ($SrTiO_3$) substrate along the (001) direction. We consider two systems (shown in Fig. 1*A*): TiO_2^{int}, where the metal–ferroelectric interface is SrO-TiO_2 and the surface termination is PbO, and PbO^{int}, where the metal–ferroelectric interface is RuO_2-PbO and the surface termination is TiO_2.

Our results reveal the role played by electrostatic, interface and surface factors in determining the polarization direction in PTO. As summarized in Fig. 1*A*, we observe that ferroelectric dipoles arise at the buffer/thin film interface (P_{int}) and at the surface (P_{surf}). The final overall polarization P is, however, independent of these local dipoles, and it arises from the interaction of the surface and interface chemistry with the electrostatic properties of the ferroelectric.

Results

Calculated Polarization in the Fully Relaxed Stoichiometric System. Our calculations show that a fully relaxed stoichiometric PTO film with a thickness over 7 u.c. on SRO presents an upward-pointing polarization P_{up} (pointing away from the substrate), irrespective of the surface/interface terminations. The relaxed u.c.-by-u.c. polarization profiles are shown in Fig. 1*B* for both the TiO_2^{int} and the PbO^{int} systems, for a representative 13-u.c.-thick PTO film (simulated on a 4-u.c.-thick SRO electrode). At the interface (bottom of the graph) the two systems have almost identical polarization which is sustained across the film. We note that the value of the polarization is $\sim 30\ \mu C/cm^2$, which is circa 40% less than the calculated bulk value of $\sim 49\ \mu C/cm^2$. This is not unexpected, as the depolarizing field quenching ultrathin polarization is still felt at this thickness, and experimentally, bulk-like polarization is not expected to emerge until ~ 30 u.c. (33). Surface effects become apparent with strong surface relaxations in the topmost five u.c. of both systems: the polarization of the topmost u.c. in the TiO_2^{int} system is $-5\ \mu C/cm^2$ and in the PbO^{int} system is $+5\ \mu C/cm^2$.

For systems with fewer than 7 u.c. the paraelectric state is the most stable, showing the existence of a critical thickness for ferroelectricity for PTO on SRO, in good agreement with previous reports on the same thin film structure (34, 35). Below this critical thickness, a metal SRO buffer at a single interface provides insufficient screening, and other interface- or surface-related effects are needed to stabilize ultrathin ferroelectricity.

We were able to stabilize configurations with downward-pointing polarization (P_{down}) but with the larger critical thickness of 11 u.c. These P_{down} systems are, however, less stable than the P_{up} (paraelectric) configuration by up to 40 meV/u.c (10 meV/u.c.).

In the following sections, we address how electrostatic, interface, and surface effects in a thin film determine the ferroelectric polarization in the relaxed film.

Electrostatic Effects. We first consider electrostatic arguments to understand the preference for P_{up} of both systems. In particular, we analyze the energy cost of screening the polar discontinuity at the free surface with electrons and holes (4).

Fig. 2a shows the u.c.-by-u.c. density of states for paraelectric TiO_2^{int} and PbO^{int} SRO/PTO/vacuum thin films. We note that the Fermi level of the SRO metal lies within the band gap of PTO, as expected from a realistic system. While the alignment itself will only be as exact as the DFT approximation underlying it, we do not have a pathological situation giving rise to unphysical spurious charge transfer (4). We are thus confident that the results of our work are physically meaningful.

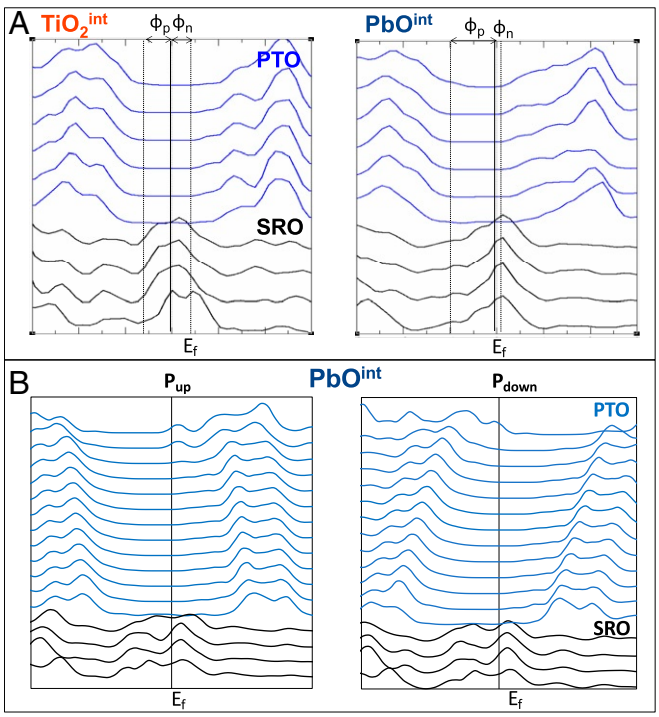

Fig. 2. (*A*) DFT-calculated projected density of states for (4 u.c. SRO)/(7 u.c. PTO)/vacuum paraelectric system. The Fermi level is the solid vertical black line, and the dotted black lines are the valence and conduction band edges. The Schottky barriers are as follows: for PbO^{int} (*Right*), $\phi_p = 1.0$ eV for holes and $\phi_n = 0.15$ eV for electrons, and for TiO_2^{int} (*Left*), $\phi_p = 0.60$ eV for holes and $\phi_n = 0.45$ eV for electrons. (*B*) The u.c.-by-u.c. density of states for a fully relaxed (4 u.c. SRO)/(13 u.c. PTO)/vacuum PbO^{int} heterostructure. SRO is in black, and PTO is in blue. The vertical black line is the Fermi energy.

The DFT-calculated Fermi level (shown as a solid black line) lies closer to the PTO conduction band than to the valence band making the Schottky barrier for electrons (ϕ_n, defined as the difference between the conduction band edge and the Fermi level) lower than that for holes (ϕ_p, defined as the difference between the Fermi level and the valence band edge). This is true for both SRO/PTO systems but especially for PbO^{int} which has $\phi_p = 1.0$ eV for holes and $\phi_n = 0.15$ eV for electrons; for TiO_2^{int} the difference between the two barriers is not as large, them being $\phi_p = 0.60$ eV for holes and $\phi_n = 0.45$ eV for electrons. Thus, a higher potential energy barrier needs to be overcome to screen the surface polarization with valence-band holes (for P_{down}) than with conduction-band electrons (for P_{up}), making the P_{up} systems more energetically favorable than the P_{down}. This is shown, for PbO^{int} (TiO_2^{int} shows a similar behavior), in Fig. 2*B*, where the u.c.-by-u.c. density of state of upward and downward polarized PbO^{int} systems is reported. We indeed see that for P_{up} the bands are less bent than in P_{down}, indicating a lower Schottky barrier for the former.

Having established the role of the band alignment and electrostatics in defining the ferroelectric polarization in a SRO/PTO thin film, we now analyze other factors which could determine the sign and magnitude of P: the interface and surface chemistry.

Role of the Epitaxial Interface. The importance of interface chemistry in stabilizing buffer/film interface dipoles has previously been shown for a number of metal–oxide interfaces [e.g., Pt/$BaTiO_3$ (34), Al, Mg, Mo, Pt, and Ag/MgO (36, 37)]. Dipole formation at the interface between a metal and an oxide has been correlated to charge transfer between the two materials (36, 37), to the stiffness of interfacial bonds (34), or to the charge mismatch at the interface (20). In this section we show that the local chemistry between SRO and PTO favors a specific polarization direction in the PbO^{int} system. This is a consequence of the formation of an interface dipole with associated charge transfer which is shown in Fig. 1*A* as P_{int}.

We isolated the influence of the interface chemistry on the FE polarization by considering in our calculations only the effect of interfacial bonding on the total energy. We employed (4 u.c. SRO)/(13 u.c. PTO)/vacuum slabs which were optimized in a paraelectric (PE) configuration. We did this for both the TiO_2^{int} and PbO^{int} systems. We next displaced the atoms in the SRO/PTO interface bilayer, explicitly shown in the cartoons in Fig. 3, by a small distance (δ) along the direction perpendicular to the interface. We then tracked the change in the total energy, $E_{\delta-PE}$, between the structure with the δ displacement and the fully paraelectric one. The graphs at the bottom of Fig. 3*A* show that the δ displacements around the paraelectric equilibrium point (the 0 in the horizontal axis) have little effect in the TiO_2^{int} system. Indeed, for the SrO-TiO_2 interface, the atoms in the SrO layer are at their most stable in the paraelectric configuration (yellow and dashed red line), while the TiO_2 layer favors rumpling by displacement of the oxygen atoms (solid red line), and upward or downward displacements are equally energetically favorable within the precision of our calculations. In contrast, in the PbO^{int} system (Fig. 3*B*), the atoms in the PbO layer favor a net downward-pointing dipole, as shown in the cartoon at the top of the figure. Indeed the blue line (corresponding to Pb) in the graph in Fig. 3*B* shows a preferential shift of Pb toward the interface, and the solid red line (corresponding to the O atom) shows a preferential upward shift of O. In the RuO_2 layer the O atoms (dashed red line) are on a saddle point, and the energies for displacing toward or away from the FE layer are comparable.

To investigate the possible link between interface rumpling and charge transfer (36, 37), we look at the deviation of the charges of the interface atoms from their bulk values in the paraelectric structure. Small changes (of $< \pm 0.05$ e/atom) are observed in the atoms at the SrO-TiO_2 interface; on the contrary, a large positive change of $+0.2$ e/atom is found for the Ru atom in the RuO_2-PbO interface. We have already pointed out that the two systems differ in the height of the electron Schottky barrier, which is low in the PbO^{int} system (Fig. 2*A*), thus promoting electron migration from the metal to the oxide. These results support the idea of a connection between interfacial charge transfer and polarization (36): the neutral SrO-TiO_2 interface has a very small preference for an upward-pointing polarization direction, while, in PbO^{int}, the positively charged RuO_2 layer promotes a P_{down} dipole in PbO.

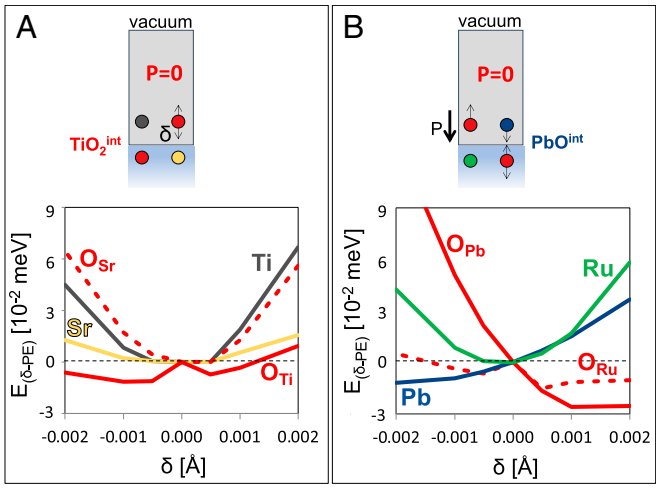

Fig. 3. (*Top*) Cartoons of the paraelectric SRO/PTO/vacuum slabs. Only the atoms at the SRO/PTO interface are explicitly shown. The arrows show the preferential direction of the displacement of the interfacial atoms away from the paraelectric structure. (*A*) The structure with TiO_2^{int} interfaces and (*B*) the structure with PbO^{int} interfaces. (*Bottom*) Relative energy of the paraelectric (4 u.c. SRO)/(13 u.c. PTO)/vacuum slabs upon δ displacements of specified interface atoms. $E_{\delta-(PE)}$ is calculated as the difference between the system with δ displacements and the fully paraelectric one.

It is worth noting that we observe this interfacial charge transfer in the paraelectric system and not in the ferroelectric structure of Fig. 1, showing that it occurs only when the ferroelectricity is suppressed. Correspondingly, we do not observe the full downward-pointing P_{int} in the ferroelectric PbO^{int} system; however, the chemical interface effect is still present in some measure, and it leads to a small reduction of the interfacial polarization with respect to the middle of the film, as seen in the blue line in Fig. 1*B*.

Thus, we have shown that the chemistry of the interface can favor a preferential direction of the polarization at the interface, shown in Fig. 1*A* as P_{int}. This interface contribution does not affect the overall direction of the polarization, but it leads to a reduction of P at the interface in the PbO^{int} system. We next investigate the role surface relaxations in determining the value and direction of P.

Surface Structure and Chemistry. We now turn our attention to the PTO/vacuum interface. We consider (4 u.c. SRO)/(13 u.c. PTO)/vacuum heterostructures (for both interfaces and polarization directions) with fixed constant polarization throughout their thickness. We progressively relax all of the u.c. from the top, and in Fig. 4*A* we plot the evolution of the energy of the four heterostructures as a function of the number of relaxed u.c. (N). The plotted energy, E_{FE-PE}, is the total energy of the systems minus the energy of the corresponding paraelectric structure. The results presented in Fig. 4*A* show that the P_{up} polarization

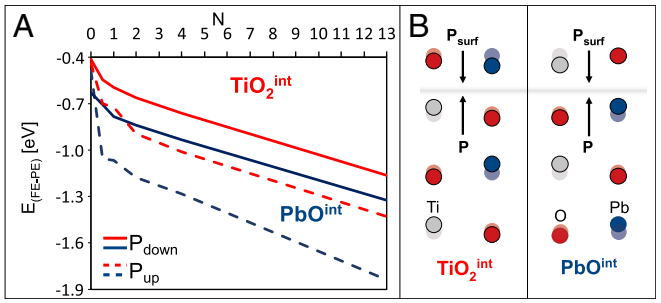

Fig. 4. (*A*) Relative stability of partially relaxed SRO/PTO/vacuum structures with respect to the paraelectric phase, E_{FE-PE}. N is the number of u.c. from the surface which are relaxed. (*B*) Schematic representation of the surface relaxations for P_{up} systems where only the topmost layer (0.5 u.c.) is relaxed. Pb is in blue, Ti is in gray, and O is in red. The arrows represent the direction of the polarization above (P_{surf}) and below (P) the gray line.

direction (dashed lines) is the most stable throughout, starting from the relaxation of the topmost surface layer (i.e., 0.5 u.c.). The energy difference between P_{up} and P_{down} is also almost constant throughout, showing that these relaxations do not affect the stability of P_{up}.

In all systems, regardless of termination and polarization direction, we observe the formation of a downward-pointing dipole in the topmost layer (Fig. 4*B*). Indeed, in the TiO_2^{int} system (Fig. 4*B*, *Left*), the stereochemical activity of the Pb lone pair, which is facing the vacuum, strongly pushes the Pb ion down toward the TiO_2 layer. In the PbO^{int} system (Fig. 4*B*, *Right*), shrinking of the Ti-O bond (38) lowers the Ti atom toward the PbO layer.

This downward-pointing surface dipole, driven by the surface chemistry, still does not reverse the overall upward-pointing polarization of the film. Indeed, despite the surface and, in the case of PbO^{int}, also the interface favoring a downward direction of the ferroelectric polarization, an upward-pointing polarization is energetically more stable for both interface types (Fig. 1). We can conclude, then, that the local chemistry at the surface and interface does not determine the overall polarization direction.

It is, however, known, following the work of ref. 39, that the band alignment between a metal and an insulator depends on the interface properties of the two. As already discussed, and shown in Fig. 2*A*, the relative position of the conduction and valence band with respect to the Fermi level is different for the two interface structures, PbO^{int} and TiO_2^{int}. It can thus be argued that it is indeed the interface which sets the polarization direction for PTO thin films on SRO, not through the local chemistry and bonding but through its influence on the overall band alignment.

Having established the principles guiding the setting of the polarization direction in a stoichiometric thin film, we now analyze the effect of surface and interface defects in the screening of the surface and interface charges.

Polarization Engineering by Surface and Interface Defects. Surface and interface defects, as well as surface adsorbates from the environment, are a common occurrence in crystalline systems. In this section we examine their effect on the structure of a ferroelectric thin film. We consider three representative scenarios: surface adsorbates and defects (Fig. 5*A*, *i*), interface defects (Fig. 5*A*, *ii*), and the simultaneous occurrence of the two (Fig. 5*A*, *iii*). Note that in this section we do not present a complete study of the defect chemistry of PTO, which would include also charged defects or defect dipoles (40), but we only consider neutral point defects whose intrinsic formal charge might be able to stabilize the ferroelectric polarization.

Surface ionic charges, occurring through defect formation or adsorption processes, interact with the ferroelectric bound charges (Fig. 5*A*, *i*) and can either screen (13, 14, 27) or enhance the depolarizing field (5, 31). Indeed, in our calculations we observe that adsorbates or defects with an associated negative charge (such as OH^- adsorbates, O^{2-} adatoms, or cation vacancies) stabilize P_{up}, regardless of the polarization direction of the initial system. Conversely, positively charged species (such as H^+ adsorbates, Pb^{2+}, Ti^{4+} adatoms, or O vacancies) favor P_{down}. A full list of the defects that we have tested is available in *SI Appendix*. The resulting polarization is robust and bulk-like throughout the film thickness: it does not suffer from either the surface effects or depolarizing field effects observed in Fig. 1*B*. We observe bulk-like polarization even in the ultrathin regime, down to a single u.c. for surface-screened systems, far below the critical thickness for PTO on SRO.

Similarly, interface defects (Fig. 5*A*, *ii*) contribute to the screening of the interface bound charges. It has been proposed in previous work that a combination of screening from the metal buffer and from interface defects can stabilize ferroelectricity in ultrathin systems (13, 14). This effect was observed in calculations performed on SRO/PTO or $SrTiO_3$/PTO heterostructures. However, in our calculations with the uncompensated top surface, we found stabilization of the ferroelectric polarization by interface defects only in the u.c. below where they are positioned. In a 3-u.c.-thick PTO film, for O (Pb, Ti) vacancies in the

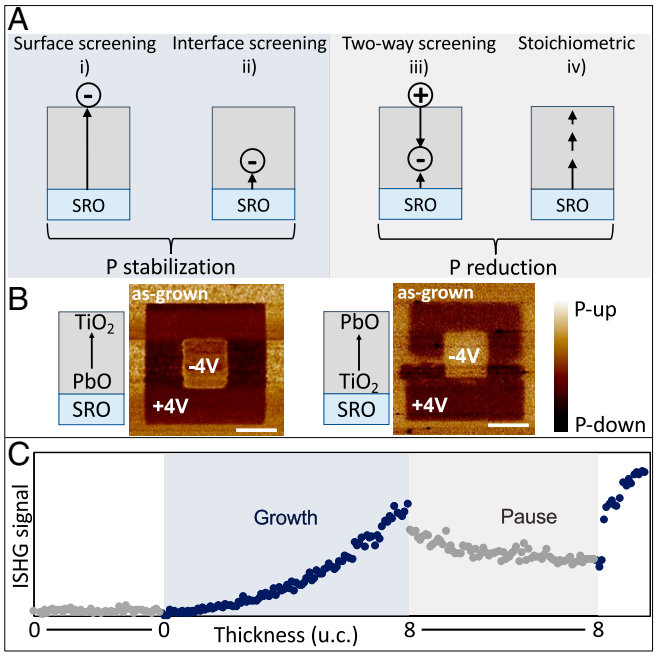

Fig. 5. (*A*) Schematic representations of the effect of surface and interface charges on the polarization. These charges could be defects or, on the surface, adsorbates. SRO is light blue, and PTO is gray. The black arrows represent the ferroelectric polarization. We consider three types of screening: (*i*) surface, (*ii*) interface, and (*iii*) a superposition of the two. (*iv*) The stoichiometric system for comparison. The blue (gray) shading indicates processes which stabilize (reduce) the polarization and are related to the mechanisms also shaded in blue (gray) of *C*. (*B*) Out-of-plane piezoresponse force microscopy phase images. The as-grown state is up-polarized (bright contrast). The polarization direction is switched down (dark contrast) after applying a +4 V bias. The reversibility of the switching is shown after successive +4 V and −4 V application in a box-in-box configuration. (Scale bar, 1 μm.) (*C*) ISHG data for the PLD growth of an SRO/PTO system. The data are in arbitrary units. The blue-shaded area corresponds to PLD growth of the PTO film, and the gray-shaded area corresponds to a pause in the growth.

interface PTO u.c. we observe P_{down} (P_{up}) polarization for the u.c. below the vacancy and paraelectric PTO above (Fig. 5*A*, *ii*). Thus, interface defects appear to be less effective at stabilizing the ferroelectric polarization for the whole film. It is important to note that a more complex distribution of defects than that calculated here, such as defect gradients (41), could occur in the film. More pronounced screening effects could be observed in that scenario. Finally, a combination of screening from the surface and the interface could occur at the same time (Fig. 5*A*, *iii*). If both contributions promote the same direction of the ferroelectric polarization, the result is a thin film with robust bulk-like polarization through the entire thickness. Alternatively, if they promote opposite directions of the polarization, as shown in Fig. 5*A*, *iii*, two regions of opposite polarization occur in the film.

In this work we have thus identified four types of surface and interface structures, two of which promote stabilization of the ferroelectric polarization (surface and interface nonstoichiometry; Fig. 5*A*, *i* and *ii*) and two a reduction of the polarization in the thin film with respect to the bulk (noncooperative defects and stoichiometric system; Fig. 5*A*, *iii* and *iv*). Our analysis indicates that engineering of surface and interface screening through adsorbates or defects could be a powerful tool to control the polarization (5, 28, 42, 43).

As a test of our theoretical predictions, we grow PTO thin films on SRO by means of PLD, and we analyze the surface and interface effects in this experimental system. PTO is ferroelectric during growth (44), and we probe the polarization as it develops using ISHG (21, 26). This technique allows us to monitor the evolution of the overall ferroelectric polarization and indirectly see the contribution of surfaces and interfaces during growth. First, we note that the polarization direction of the films after growth is P_{up} for both the TiO_2^{int} and PbO^{int} systems as expected from our theoretical predictions. This can be seen in Fig. 5*B* which shows piezoresponse force microscopy measurements for the two systems. The external area of the sample shows that the as-grown film is P_{up} polarized. The local application of an electric field using the scanning probe tip (± 4 V bias) can affect the surface charges or the film stoichiometry and therefore stabilize the P_{down} state (45). Both TiO_2^{int} and PbO^{int} films are fully switchable. This is consistent with our theoretical results showing that applying a positive charge to the surface of both TiO_2^{int} and PbO^{int} systems leads to a reversal of the polarization direction from P_{up} to P_{down} (*SI Appendix*, Fig. S5 and Table S1).

The polarization measured during thin film growth with ISHG can be seen in Fig. 5*C*. Data points during growth are shown in blue, and data points while the growth is paused are in gray. The ISHG signal, which is proportional to the square of the polarization, shows that the onset of polarization—corresponding to a nonzero ISHG signal in the blue data in Fig. 5*C*—occurs shortly after the beginning of the deposition, indicating very small or no critical thickness. After the end of growth, a drop in the total value of the polarization is observed (gray data points in Fig. 5*C*); however, the full strength of the polarization is swiftly recovered when growth is resumed (Fig. 5*C*, blue data points on the right), indicating that the observed effect is not the result of domain splitting but likely surface-related.

In light of the screening models of Fig. 5*A*, we attribute the absence of critical thickness in PTO to either screening from both the SRO/PTO interface and the top surface (Fig. 5*A*, *i*) or to a defect-rich SRO/PTO interface (Fig. 5*A*, *ii*). When growth is interrupted, the chemistry inside the PLD chamber changes, affecting the surface structure. The decrease in polarization upon interruption of growth can then be related to the polarization-reducing mechanisms in Fig. 5*A*, *iii* and *iv*. That is, the surface can lose the screening mechanism and become stoichiometric, with a polarization of the topmost u.c. shifting from bulk-like to surface-relaxed (Fig. 5*A*, *iv*). Alternatively, the surface polarization is partially reversed by surface effects as in Fig. 5*A*, *iii*.

Summary

In this work, we have determined the factors that influence the polarization for ferroelectric PTO thin films on an SRO metallic buffer. We have shown that the interplay of electronic structure and the chemistry of the surface and the interface is key to determining the overall polarization. In particular, the engineering of specific surface and interface defects could be a powerful way to to select the polarization direction and achieve bulk-like polarization strength across the film thickness.

We predicted and obtained experimental confirmation that PTO thin films grown on an SRO buffer have a strong preference for an upward-pointing polarization. This is a result of the interfacial band alignment between SRO and PTO which results in a lower Schottky barrier for electrons and, in turn, a lower energy cost for screening the positive surface polarization charge with electrode electrons.

We have also shown that surface defects and adsorbates can dramatically alter the polarization and can be engineered both to screen the surface polar discontinuity and to reverse the polarization direction (Fig. 5). With our calculations we identified a mechanism which could lead to a thin film with robust bulk-like polarization across its thickness through a combination of surface and interface defects. Our experimental results are compatible with the theoretical scenarios and reveal the key role of defects and adsorbates during epitaxial thin film growth in enhancing or suppressiong the FE polarization.

We hope that our findings motivate further experimental work toward the engineering of thin films with bulk-like polarization. For example, careful analysis of the defect structure of the film could help pinpoint the exact stabilization/reduction mechanism at play during epitaxial growth. In turn, this could enable the promotion of a structure with enhanced ferroelectric polarization by tuning the experimental conditions. We also predict that this same screening mechanisms which suppresses the upward-pointing polarization after growth in Fig. 5*C* could, on the contrary, lead to an enhancement of the ferroelectric polarization with a downward-pointing ferroelectric polarization. Verification of this prediction would require finding a substrate which favors P_{down} PTO.

Materials and Methods

Experimental. We study the polarization state of PTO in PTO/SRO heterostructures depending on the PTO top layer plane being either TiO_2 or PbO. Uniaxial FE PTO (001) films with a thickness of 25 u.c. were grown by PLD on (001)-oriented $SrTiO_3$ buffered by 10 u.c. of SRO. The SRO thickness is enough to ensure it is metallic and thus provides screening. SRO/PTO systems with insulating (ultrathin) SRO show a different and complex behavior and have been studied in ref. 46. The laser fluence, its repetition rate, substrate temperature, and growth pressure for individual layers were as follows: SRO, 0.9 Jcm^{-2}, 2 Hz, 700°C, and 0.1 mbar O_2; PTO, 1.15 Jcm^{-2}, 4 Hz, 550°C, and 0.12 mbar O_2; and TiO_2: 1.15 Jcm^{-2}, 2 Hz, 550°C, and 0.12 mbar O_2. The substrate exerts $\sim$1.4% compressive strain, increasing the FE Curie temperature above the growth temperature (T_{growth} = 550° C). We monitor the FE response during the thin film deposition using ISHG as a noninvasive detection technique. SHG denotes frequency doubling of a light wave in a material. This process is sensitive to the loss of inversion symmetry that occurs with the emergence of FE order (21, 47). The ISHG light is measured in 45° reflection geometry, and its polarization is chosen such that it detects the out-of-plane component of the FE polarization emerging in the PTO during the deposition process (32). Room-temperature FE properties were confirmed using piezoresponse force microscopy. The thin film piezoresponse was characterized using a Bruker Multimode 8 microscope. An alternating voltage of 0.5 V was applied between the tip and the SRO bottom electrode to access the ferroelectric polarization direction. When poling an area, the alternating voltage was switched off, and only the ± 4 V DC bias was applied to the tip, while the bottom electrode was

grounded. Both films show up-polarized as-grown state and repeatable switching (Fig. 5*C*).

PTO (001) u.c. consist of PbO-TiO_2 planes. The growth mode established during the PLD process requires that the smallest building unit corresponds to a full u.c.; thus, necessarily, a PTO system with a TiO_2 interface has a PbO surface and vice versa. TiO_2^{int} is the only system accessible to our experiments as the RuO_2 layer is volatile, and therefore, PLD of PTO necessarily starts with a TiO_2 layer (48). Experimentally, a system with a PbO^{int} surface was engineered by depositing a thin TiO_2 layer on top of the SrO-terminated SRO. Results for this system are similar to the TiO_2^{int} one and are presented in *SI Appendix*.

Theory. Density functional theory calculations were carried out with the VASP (49–51) package (version 5.4.1) using the PBEsol (52) functional which gives a good metal/insulator band alignment at the interface, with the Fermi level of the metal falling within the PTO gap. Core electrons were replaced by projector augmented wave potentials (53), whereas the valence states (10 electrons for Sr, 4 for Pb, 8 for Ru, 4 for Ti, and 6 for O) were expanded in plane waves with a cutoff energy of 500 eV. A Monkhorst–Pack grid of $6 \times 6 \times 1$ *k* points was used for all thin films with a surface area of 1×1 u.c. Note that the surface area of 1 u.c. does not allow for domain formation, so this effect was not explored in this work. Moreover, they do not allow the antiferrodistortive reconstruction which has been observed for PTO (001) (54, 55) to occur. In principle, changes in rotations and tilts can affect the ferroelectricity of a material (56). Tests on a 13-u.c. PbO_{int} slab with a 2×2 unit area show that the polarization profile between the system in Fig. 1 and one with the surface reconstruction are very similar, showing that the distortions have only a small effect on the polarization (*SI Appendix*).

We added a 4-u.c.-thick SRO electrode under the PTO slab. We considered PTO slab thicknesses between 3 and 13 u.c. Periodic images were separated by ~ 15 Å of vacuum in the direction perpendicular to the surface. We did not explicitly simulate the $SrTiO_3$ substrate; instead we used the $SrTiO_3$ lattice parameter as the in-plane lattice constant for the SRO/PTO thin film structure ($a_{PBEsol} = 3.905$ Å). A dipole correction along the direction perpendicular to the surface was applied. Geometry optimizations were performed with a residual force threshold of 0.005 eV/Å, and the threshold for energy convergence in the self-consistent cycle was 10^{-6} eV/Å. All visualization of the atomistic systems has been produced with the Visualization for Electronic and STructural Analysis (VESTA) software (57).

In order to optimize a paraelectric system we first simulated an SRO/PTO heterostructure (without vacuum) and imposed a mirror plane in the middle of PTO (8, 34). We then relaxed the ionic positions to obtain the lowest energy (paraelectric) structure within this constraint. Once the optimization of the heterostructure was completed, we added vacuum at one interface.

Calculations of defects were performed on SRO/PTO/vacuum slabs, with the PTO thickness varying from 1 to 13 u.c. We added a concentration of surface defects sufficient to compensate the surface charge density of 0.75 e/A, where A is the unit surface area. Therefore, we considered u.c. with the following surface areas: 1×1 u.c. for H adatoms, 1×2 and 2×2 u.c. for Pb and O adatoms/vacancies, and 2×2 u.c. for Ti adatoms/vacancies. Representative structures are shown in *SI Appendix*, and the coordinates are provided in CIF format.

Data Availability. All study data are included in the article and *SI Appendix*.

ACKNOWLEDGMENTS. C.G. is supported by the European Union (EU)'s Horizon 2020 research and innovation program under the Marie Skłodowska-Curie grant agreement 744027. C.G.'s computational work was supported by a grant from the Swiss National Supercomputing Centre (CSCS) under project ID s870. N.S., M.T., and M.F. acknowledge support by the EU European Research Council (Advanced Grant 694955—INSEETO). M.T. acknowledges financial support by the Swiss National Science Foundation under Project No. 200021_188414.

1. K. Uchino, Ferroelectric Devices, Materials Engineering (Taylor & Francis, 2000).
2. M. B. Starr, X. Wang, Fundamental analysis of piezocatalysis process on the surfaces of strained piezoelectric materials. *Sci. Rep.* **3**, 2160 (2013).
3. D. D. Fong *et al.*, Stabilization of monodomain polarization in ultrathin $PbTiO_3$ films. *Phys. Rev. Lett.* **96**, 127601 (2006).
4. M. Stengel, Electrostatic stability of insulating surfaces: Theory and applications. *Phys. Rev. B* **84**, 205432 (2011).
5. R. V. Wang *et al.*, Reversible chemical switching of a ferroelectric film. *Phys. Rev. Lett.* **102**, 047601 (2009).
6. M. J. Highland *et al.*, Equilibrium polarization of ultrathin $PbTiO_3$ with surface compensation controlled by oxygen partial pressure. *Phys. Rev. Lett.* **107**, 187602 (2011).
7. J. F. Scott, Future issues in ferroelectric miniaturization. *Ferroelectrics* **206**, 365–379 (1997).
8. J. Junquera, P. Ghosez, Critical thickness for ferroelectricity in perovskite ultrathin films. *Nature* **422**, 506–509 (2003).
9. K. Ishikawa, T. Nomura, N. Okada, K. Takada, Size effect on the phase transition in $PbTiO_3$ fine particles. *Jap. J. Appl. Phys.* **35**, 5196–5198 (1996).
10. N. Sai, A. M. Kolpak, A. M. Rappe, Ferroelectricity in ultrathin perovskite films. *Phys. Rev. B* **72**, 020101 (2005).
11. M. Q. Cai, Y. Zheng, P. W. Ma, C. H. Woo, Vanishing critical thickness in asymmetric ferroelectric tunnel junctions: First principle simulations. *J. Appl. Phys.* **109**, 024103 (2011).
12. L. Despont *et al.*, Direct evidence for ferroelectric polar distortion in ultrathin lead titanate perovskite films. *Phys. Rev. B* **73**, 094110 (2006).
13. P. Gao *et al.*, Possible absence of critical thickness and size effect in ultrathin perovskite ferroelectric films. *Nat. Commun.* **8**, 15549 (2017).
14. M. F. Chisholm, W. Luo, M. P. Oxley, S. T. Pantelides, H. N. Lee, Atomic-scale compensation phenomena at polar interfaces. *Phys. Rev. Lett.* **105**, 197602 (2010).
15. G. Gerra, A. K. Tagantsev, N. Setter, K. Parlinski, Ionic polarizability of conductive metal oxides and critical thickness for ferroelectricity in $BaTiO_3$. *Phys. Rev. Lett.* **96**, 107603 (2006).
16. D. Puggioni, G. Giovannetti, J. M. Rondinelli, Polar metals as electrodes to suppress the critical-thickness limit in ferroelectric nanocapacitors. *J. Appl. Phys.* **124**, 174102 (2018).
17. X. T. Liu, W. J. Chen, G. L. Jiang, B. Wang, Y. Zheng, Diverse interface effects on ferroelectricity and magnetoelectric coupling in asymmetric multiferroic tunnel junctions: The role of the interfacial bonding structure. *Phys. Chem. Chem. Phys.* **18**, 2850–2858 (2016).
18. M. Stengel, D. Vanderbilt, N. A. Spaldin, Enhancement of ferroelectricity at metal–oxide interfaces. *Nat. Mater.* **8**, 392–397 (2009).
19. H. Yamada *et al.*, Strong surface-termination effect on electroresistance in ferroelectric tunnel junctions. *Adv. Funct. Mater.* **25**, 2708–2714 (2015).
20. P. Yu *et al.*, Interface control of bulk ferroelectric polarization. *Proc. Natl. Acad. Sci. U.S.A.* **109**, 9710–9715 (2012).
21. G. De Luca *et al.*, Nanoscale design of polarization in ultrathin ferroelectric heterostructures. *Nat. Commun.* **8**, 1419 (2017).
22. C. G. Duan, R. F. Sabirianov, W. N. Mei, S. S. Jaswal, E. Y. Tsymbal, Interface effect on ferroelectricity at the nanoscale. *Nano Lett.* **6**, 483–487 (2006).
23. C. Lichtensteiger *et al.*, *Oxide Ultrathin Films: Science and Technology* (Wiley, Weinheim, 2011), pp. 265–308.
24. L. W. Martin, A. M. Rappe, Thin-film ferroelectric materials and their applications. *Nat. Rev. Mater.* **2**, 16087 (2017).
25. M. Setvin *et al.*, Polarity compensation mechanisms on the perovskite surface $KTaO_3$ (001). *Science* **359**, 572–575 (2018).
26. N. Strkalj *et al.*, Depolarizing-field effects in epitaxial capacitor heterostructures. *Phys. Rev. Lett.* **123**, 147601 (2019).
27. S. V. Levchenko, A. M. Rappe, Influence of ferroelectric polarization on the equilibrium stoichiometry of lithium niobate (0001) surfaces. *Phys. Rev. Lett.* **100**, 256101 (2008).
28. K. Garrity, A. Kakekhani, A. Kolpak, S. Ismail-Beigi, Ferroelectric surface chemistry: First-principles study of the $PbTiO_3$ surface. *Phys. Rev. B* **88**, 045401 (2013).
29. W. A. Saidi, J. M. P. Martirez, A. M. Rappe, Strong reciprocal interaction between polarization and surface stoichiometry in oxide ferroelectrics. *Nano Lett.* **14**, 6711–6717 (2014).
30. L. C. Tănase *et al.*, Ferroelectric triggering of carbon monoxide adsorption on lead zirco-titanate (001) surfaces. *Sci. Rep.* **6**, 35301 (2016).
31. Y. Tian *et al.*, Water printing of ferroelectric polarization. *Nat. Commun.* **9**, 3809 (2018).
32. J. Nordlander, G. De Luca, N. Strkalj, M. Fiebig, M. Trassin, Probing ferroic states in oxide thin films using optical second harmonic generation. *Appl. Sci.* **8**, 570 (2018).
33. C. Lichtensteiger, J. M. Triscone, J. Junquera, P. Ghosez, Ferroelectricity and tetragonality in ultrathin $PbTiO_3$ films. *Phys. Rev. Lett.* **94**, 047603 (2005).
34. M. Stengel, D. Vanderbilt, N. A. Spaldin, Enhancement of ferroelectricity at metal–oxide interfaces. *Nat. Mater.* **8**, 392–397 (2009).
35. R. Dorin, L. D. Filip, L. Pintilie, K. T. Butler, N. Plugaru, Designing functional ferroelectric interfaces from first-principles: Dipoles and band bending at oxide heterojunctions. *New J. Phys.* **21**, 113005 (2019).
36. J. Goniakowski, C. Noguera, Polarization and rumpling in oxide monolayers deposited on metallic substrates. *Phys. Rev. B* **79**, 155433 (2009).
37. J. Goniakowski, C. Noguera, Electronic states and Schottky barrier height at metal/MgO(100) interfaces. *Interface Sci.* **12**, 93–103 (2004).
38. K. Kern, "Restructuring at surfaces" in *Surface Science*, R. F. Howe, R. N. Lamb, K. Wandelt, Eds. (Springer, Berlin, 1993), pp. 81–94.
39. M. Stengel, P. Aguado-Puente, N. A. Spaldin, J. Junquera, Band alignment at metal/ferroelectric interfaces: Insights and artifacts from first principles. *Phys. Rev. B* **83**, 235112 (2011).
40. E. Cockayne, B. P. Burton, Dipole moment of a Pb-O vacancy pair in $PbTiO_3$. *Phys. Rev. B* **69**, 144116 (2004).
41. C. Weymann *et al.*, Full control of polarisation in ferroelectric thin films using growth temperature to modulate defects. *Adv. Electron. Mater.*, in press.
42. L. Xie *et al.*, Giant ferroelectric polarization in ultrathin ferroelectrics via boundary-condition engineering. *Adv. Mater.* **29**, 1701475 (2017).
43. H. Béa *et al.*, Influence of parasitic phases on the properties of $BiFeO_3$ epitaxial thin films. *Appl. Phys. Lett.* **87**, 072508 (2005).

44. D. D. Fong *et al.*, Ferroelectricity in ultrathin perovskite films. *Science* **304**, 1650–1653 (2004).
45. N. Domingo *et al.*, Surface charged species and electrochemistry of ferroelectric thin films. *Nanoscale* **11**, 17920–17930 (2019).
46. S. J. Callori *et al.*, Ferroelectric $PbTiO_3/SrRuO_3$ superlattices with broken inversion symmetry. *Phys. Rev. Lett.* **109**, 067601 (2012).
47. V. A. Stoica *et al.*, Optical creation of a supercrystal with three-dimensional nanoscale periodicity. *Nat. Mater.* **18**, 377–383 (2019).
48. G. Rijnders, D. H. A. Blank, J. Choi, C. B. Eom, Enhanced surface diffusion through termination conversion during epitaxial $SrRuO_3$ growth. *Appl. Phys. Lett.* **84**, 505–507 (2004).
49. G. Kresse, J. Furthmuller, Efficiency of ab-initio total energy calculations for metals and semiconductors using a plane-wave basis set. *Comput. Mater. Sci.* **6**, 15–50 (1996).
50. G. Kresse, J. Furthmuller, Efficient iterative schemes for *ab initio* total-energy calculations using a plane-wave basis set. *Phys. Rev. B* **54**, 11169–11186 (1996).
51. G. Kresse, J. Hafner, *Ab initio* molecular dynamics for liquid metals. *Phys. Rev. B* **47**, 558–561 (1993).
52. J. P. Perdew *et al.*, Restoring the density-gradient expansion for exchange in solids and surfaces. *Phys. Rev. Lett.* **100**, 136406 (2008).
53. G. Kresse, D. Joubert, From ultrasoft pseudopotentials to the projector augmented-wave method. *Phys. Rev. B* **59**, 1758–1775 (1999).
54. J. He, G. B. Stephenson, S. M. Nakhmanson, Electronic surface compensation of polarization in $PbTiO_3$ films. *J. Appl. Phys.* **112**, 054112 (2012).
55. C. Bungaro, K. M. Rabe, Coexistence of antiferrodistortive and ferroelectric distortions at the $PbTiO_3$ (001) surface. *Phys. Rev. B* **71**, 035420 (2005).
56. D. I. Bilc, D. J. Singh, Frustration of tilts and *a*-site driven ferroelectricity in $KNbO_3-LiNbO_3$ alloys. *Phys. Rev. Lett.* **96**, 147602 (2006).
57. K. Momma, F. Izumi, *VESTA3* for three-dimensional visualization of crystal, volumetric and morphology data. *J. Appl. Crystallogr.* **44**, 1272–1276 (2011).